British Journal of Pharmacology

DOI:10.1111/j.1476-5381.2011.01483.x
www.brjpharmacol.org

RESEARCH PAPER

# Characteristics and molecular basis of celecoxib modulation on $K_v7$ potassium channels

XN Du[1], X Zhang[1], JL Qi[1,2], HL An[3], JW Li[3], YM Wan[1], Y Fu[2], HX Gao[1], ZB Gao[4], Y Zhan[3] and HL Zhang[1]

[1]*The Key Laboratory of Neural and Vascular Biology, Ministry of Education, Department of Pharmacology, Shijiazhuang, China,* [2]*Department of New Drug Development, Hebei Medical University, Shijiazhuang, China,* [3]*Institute of Biophysics, Hebei University of Technology, Tianjin, China, and* [4]*Center for Drug Discovery and Design, The State Key Laboratory of Drug Research, Shanghai Institute of Materia Medica, Shanghai Institute for Biological Science, Chinese Academy of Science, Shanghai, China*

**Correspondence**
Professor Hailin Zhang, Department of Pharmacology, Hebei Medical University, No.361 East Zhongshan Road, Shijiazhuang, Hebei, 050017, China. E-mail: zhanghl@hebmu.edu.cn, or to Dr Xiaona Du: du_xiaona@yahoo.com

**Keywords**
activation of potassium channels; celecoxib; HEK 293 cell; $K_v7$; NSAIDs; retigabine; SCG

**Received**
7 January 2011
**Revised**
13 April 2011
**Accepted**
5 May 2011

## BACKGROUND AND PURPOSE

Celecoxib is a selective cyclooxygenase-2 (COX-2) inhibitor used for the treatment of pain and inflammation. Emerging and accumulating evidence suggests that celecoxib can affect cellular targets other than COX, such as ion channels. In this study, we characterized the effects of celecoxib on $K_v7$ $K^+$ channels and compared its effects with the well-established $K_v7$ channel opener retigabine.

## EXPERIMENTAL APPROACH

A perforated whole-cell patch technique was used to record $K_v7$currents expressed in HEK 293 cells and M-type currents from rat superior cervical ganglion neurons.

## KEY RESULTS

Celecoxib enhanced $K_v7.2$–7.4, $K_v7.2/7.3$ and $K_v7.3/7.5$ currents but inhibited $K_v7.1$ and $K_v7.1$/KCNE1 currents and these effects were concentration dependent. The $IC_{50}$ value for inhibition of $K_v7.1$ channels was approximately 4 μM and the $EC_{50}$ values for activation of $K_v7.2$–7.4, $K_v7.2/K_v7.3$ and $K_v7.3/K_v7.5$ channels were approximately 2–5 μM. The effects of celecoxib were manifested by increasing current amplitudes, shifting the voltage-dependent activation curve in a more negative direction and slowing the deactivation of $K_v7$ currents. 2,5-Dimethyl-celecoxib, a celecoxib analogue devoid of COX inhibition activity, has similar but greater effects on $K_v7$currents. $K_v7.2$(A235T) and $K_v7.2$(W236L) mutant channels, which have greatly attenuated responses to retigabine, showed a reversed response to celecoxib, from activation to inhibition.

## CONCLUSIONS AND IMPLICATIONS

These results suggest that $K_v7$ channels are targets of celecoxib action and provide new mechanistic evidence for understanding the effects of celecoxib. They also provide a new approach to developing $K_v7$ modulators and for studying the structure–function relationship of $K_v7$ channels.

## Abbreviations

NSAIDs, non-steroidal anti-inflammatory drugs; SCG, superior cervical ganglion

## Introduction

The introduction of selective cyclooxygenase-2 (COX-2) inhibitors into the market was considered to be a major improvement on traditional non-steroidal anti-inflammatory drugs (NSAIDs) for the treatment of pain and inflammation. These COX-2 inhibitors were expected to be safer due to the lack of gastrointestinal and other NSAID side effects associated with inhibition of COX-1 (Flower, 2003). However, the safety of selective COX-2 inhibitors was soon in question, as rofecoxib, but not celecoxib, both selective COX-2 inhibitors, was shown to significantly increase the risk of cardiovascular events (McGettigan and Henry, 2006; White *et al.*, 2007).

The factors that distinguish celecoxib from rofecoxib and other selective COX-2 inhibitors are still a matter for debate. One possible explanation is that some beneficial effects of celecoxib may antagonize the deleterious effects inherent in COX-2 inhibitors. Indeed, patients receiving celecoxib have a significantly lower risk of developing hypertension compared with those receiving rofecoxib (Cho *et al.*, 2003; Aw *et al.*, 2005). Emerging and accumulating evidence suggests that celecoxib can affect cellular targets other than COX. Ion channels are prominent among these non-COX targets as new candidates for the molecular basis of some of the actions of celecoxib. In this regard, recent work by Brueggemann and colleagues proposes the interesting and attractive hypothesis that the beneficial effects of celecoxib on the cardiovascular system may result from its actions on two types of ion channels, the $K_v7$ potassium and L-type calcium channels (Brueggemann *et al.*, 2009, see also Shapiro, 2009; channel nomenclature follows Alexander *et al.*, 2009). Celecoxib, but not rofecoxib or diclofenac, enhanced $K_v7$ (possibly $K_v7.5$) and suppressed L-type voltage-sensitive calcium currents in A7r5 rat aortic smooth muscle cells and freshly isolated rat mesenteric artery myocytes (Brueggemann *et al.*, 2009). This study also showed that celecoxib, but not rofecoxib, inhibited calcium responses to vasopressin in A7r5 cells and dilated intact and endothelium-denuded rat mesenteric arteries. The authors concluded that these effects were independent of COX-2 inhibition and may explain the differential risk of cardiovascular events in patients taking different selective COX-2 inhibitors (Brueggemann *et al.*, 2009).

*KCNQ* genes encode $K^+$ channel subunits of the $K_v7$ family. There are five members of this family: $K_v7.1$ to $K_v7.5$ (corresponding to *KCNQ1–KCNQ5*). Of these members, four ($K_v7.2$– $K_v7.5$) are expressed in the nervous system (Jentsch, 2000; Robbins, 2001). $K_v7.2$ and $K_v7.3$ are the principal subunit components of the slow, voltage-gated M-channel, which widely regulates neuronal excitability, although other subunits may contribute to M-type currents in some locations (Brown and Passmore, 2009). In vascular smooth muscle cells, the discovery of several $K_v7$ subtypes raises the possibility of controlling vascular tone by M-channel activity (Mackie and Byron, 2008). Indeed, $K_v7.1$, $K_v7.4$ and $K_v7.5$ channels have all been identified in vascular smooth muscle cells (Yeung *et al.*, 2007; Zhong *et al.*, 2010), and $K_v7$ channel activity seems instrumental to the vasoconstrictive response to the hormone arginine vasopressin (Mackie *et al.*, 2008; Brueggemann *et al.*, 2009) or to phenylephrine (Yeung *et al.*, 2007). The $K_v7.1$ channel is mainly expressed in cardiac myo-

**Table 1**
The effects of celecoxib and retigabine (RTG) on the voltage-dependent activation and activation and deactivation kinetics of $K_v7$ currents

| | | $K_v7.1$ | $K_v7.2$ | $K_v7.3$ | $K_v7.4$ | $K_v7.3/K_v7.5$ | $K_v7.2/K_v7.3$ | $K_v7.2(A235T)$ | $K_v7.2(W236L)$ |
|---|---|---|---|---|---|---|---|---|---|
| $\Delta V_{1/2}$ (mV) | Celecoxib (10 μM) | −5.7 ± 1.6 | −13.8 ± 0.9 | −7.8 ± 0.9 | −20.4 ± 4.2 | −7.8 ± 2.9 | −11.5 ± 2.1 | +32.3 ± 4.9 | −4.0 ± 3.2 |
| | | NS | ** | ** | ** | ** | ** | ** | NS |
| | RTG (10 μM) | −2.1 ± 1.0 | −40.0 ± 1.0 | −37.9 ± 2.1 | −27.3 ± 3.1 | −8.7 ± 2.5 | −35.6 ± 2.8 | −7.6 ± 5.1 | −3.0 ± 8.7 |
| | | NS | ** | ** | ** | ** | ** | * | NS |
| τ (activation) (ms) | Control | 255 ± 18 | 119 ± 6 | 77 ± 5 | 98 ± 17 | 121 ± 13 | 60 ± 5 | | |
| | Celecoxib (10 μM) | 318 ± 26 | 103 ± 6 | 58 ± 5 | 93 ± 15 | 105 ± 11 | 49 ± 3 | | |
| | | ** | * | ** | NS | ** | ** | | |
| τ (deactivation) (ms) | Control | 208 ± 15 | 48 ± 2 | 124 ± 5 | 60 ± 4 | 120 ± 16 | 40 ± 2 | | |
| | Celecoxib (10 μM) | 311 ± 16 | 73 ± 5 | 159 ± 9 | 90 ± 6 | 166 ± 21 | 64 ± 4 | | |
| | | ** | ** | ** | ** | ** | ** | | |

*$P < 0.05$, **$P < 0.01$ compared with the control; NS, not significant compared with the control.$\Delta V_{1/2}$ – the difference of the half-activation potential before and after treatment with celecoxib or retigabine, $\Delta V_{1/2} = V_{1/2}$ (after) – $V_{1/2}$ (before).
$n = 4–6$ for $\Delta V_{1/2}$ measurements; $n = 5–6$ for τ measurements.

cytes and the $K_v7.1$/KCNE1 channel complex that underlies the delayed rectifier potassium current, $IK_s$, is key for controlling the duration of the action potential of the human heart (Barhanin *et al.*, 1996; Sanguinetti *et al.*, 1996). The importance of $K_v7$ channels can best be assessed by the mutations in the genes for four of these subunits ($K_v7.1$– $K_v7.4$) that give rise to genetic disorders in humans (Jentsch, 2000).

Although the $K_v7.5$ subunit has been suggested as a target of celecoxib activation (Brueggemann *et al.*, 2009), a systematic study on celecoxib modulation of $K_v7$ channels is lacking. This question is worthy of investigation, considering the physiological importance of $K_v7$ channels, the wide prescription of celecoxib as a NSAID and its other potential clinical uses. In this study, we have characterized the effects of celecoxib on all members of the $K_v7$ channel family and compared its effects with the well-established $K_v7$ channel opener, retigabine, and the non-COX-inhibitor analogue, 2,5-dimethyl-celecoxib (DM-celecoxib) (Figure S1). The mechanism of action for celecoxib was also studied.

## Methods

### *cDNA constructs*

Plasmids encoding human $K_v7.1$, human $K_v7.2$, rat $K_v7.3$, human $K_v7.4$ and human $K_v7.5$ channels (GenBank accession numbers: NM000218, AF110020, AF091247, AF105202 and AF249278 respectively) were kindly provided by Diomedes E. Logothetis (Virginia Commonwealth University, Richmond, VA, USA) and subcloned into pcDNA3. Kv7.2(A235T) and Kv7.2(W236L) mutants were kindly provided by Min Li (Johns Hopkins University, Baltimore, MD, USA). $K_v7.1$(T265A) and $K_v7.1$(L266W) mutants were produced by *Pfu* DNA polymerase with a QuickChange kit (Stratagene, La Jolla, CA, USA). The structure of the mutants was confirmed with DNA sequencing.

### *HEK293 cell culture and transfection*

HEK293 cells were cultured in Dulbecco's modified Eagle's medium (DMEM) supplemented with 10% fetal bovine serum and antibiotics in a humidified incubator at 37°C (5% $CO_2$). The cells were seeded on glass coverslips in a 24-multiwell plate and transfected when 60–70% confluence was reached. For transfection of six wells of cells, a mixture of 3 μg $K_v7$ in pcDNA3 (1.5 μg cDNA for each channel subunit when two channel subunits were co-expressed), pEGFP-N1 cDNAs and 3 μL Lipofectamine 2000 reagent (Invitrogen) were prepared in 1.2 mL of DMEM and incubated for 20 min according to the manufacturer's instructions. The mixture was then applied to the cell culture wells and incubated for 4–6 h. Recordings were made 24 h after cell transfection, and the cells were used within 48 h.

### *Rat superior cervical ganglion neuron culture*

All animal care and experimental procedures were approved by the Animal Care and Ethical Committee of Hebei Medical University (Shijiazhuang, China) under policies adhering to IASP guidelines for use of animals. Superior cervical ganglia (SCGs) were isolated from 10- to 17-day-old Sprague Dawley rats, cut into pieces, transferred into a collagenase solution (1 mg·mL$^{-1}$) and incubated for 30 min at 37°C. The ganglia were then placed into trypsin solution (2.5 mg·mL$^{-1}$) for 30 min at 37°C. The digested fragments were then rinsed with 2 mL DMEM plus 10% fetal bovine serum three times, centrifuged and dissociated by trituration. The isolated cells were plated onto glass coverslips precoated with poly-D-lysine and incubated at 37°C. After the neurons had attached to the coverslips, the cell culture medium was changed to Neurobasal plus B27 supplement (Invitrogen). The neurons were cultured for 1 day and used within 24 h.

### *Electrophysiology*

For current measurements in the SCG neurons and HEK293 cells, recordings were performed using the perforated (amphotericin B, 250 μg·mL$^{-1}$, Sigma) whole-cell configuration of the patch-clamp technique. The signals were amplified using an Axon 700B patch-clamp amplifier (Axon Instruments) and filtered at 2 kHz. Patch electrodes were pulled with a Flaming/Brown micropipette puller (Sutter Instruments) and fire-polished to a final resistance of 1–2 MΩ when filled with internal solution. To reduce the errors of the voltage clamping arising from the series resistance, the $K_v7$ channels were expressed in a low level so that the maximum current amplitudes were at most cases less than 3 nA; we also used series resistance compensation which normally reached 60–80%. The access resistance in our experiments was measured to be around 7–12 Mohms. Thus, the maximum voltage errors were less than 10 mV (around a few mV in most cases). Data acquisition was achieved using the pClamp 10 software. The internal solution for the HEK293 cell and rat SCG neuron recording was as follows (in mM): 150 KCl, 5 $MgCl_2$ and 10 HEPES, adjusted to pH 7.4 with KOH. The external solution for the HEK293 cells and SCG neurons contained the following (in mM): 160 NaCl, 2.5 KCl, 2 $CaCl_2$, 1 $MgCl_2$, 10 HEPES and 10 glucose, adjusted to pH 7.4 with NaOH. The perfusion

**Figure 1**

The effects of celecoxib and retigabine on $K_v7$ currents. The whole-cell currents were recorded from HEK293 cells expressing $K_v7$ channels by using the voltage protocol shown at the top of the Figure. The current traces of homomeric $K_v7.1$–7.4 (A–D) and heteromeric $K_v7.3$/$K_v7.5$ channels (E) induced by the multiple depolarization steps were shown. The perforated whole-cell patch clamp technique was used. The cells were held at –80 mV. The arrows indicate the currents induced by the –20 mV step potential. For each cell, the effects of 10 μM celecoxib and 10 μM retigabine (RTG) on $K_v7$ currents were tested. Either celecoxib or retigabine was applied first and the second drug was always applied after the first drug had been washed out (3–5 min). Celecoxib and retigabine were applied until the effects were stabilized, normally 1–3 min. (F) Normalized current amplitudes at –20 mV. The stead state current amplitudes were measured at the end of the depolarizing steps. *$P < 0.05$, **$P < 0.01$, compared with the current amplitudes in the absence of celecoxib, which were taken as 1. $n = 5$–8.

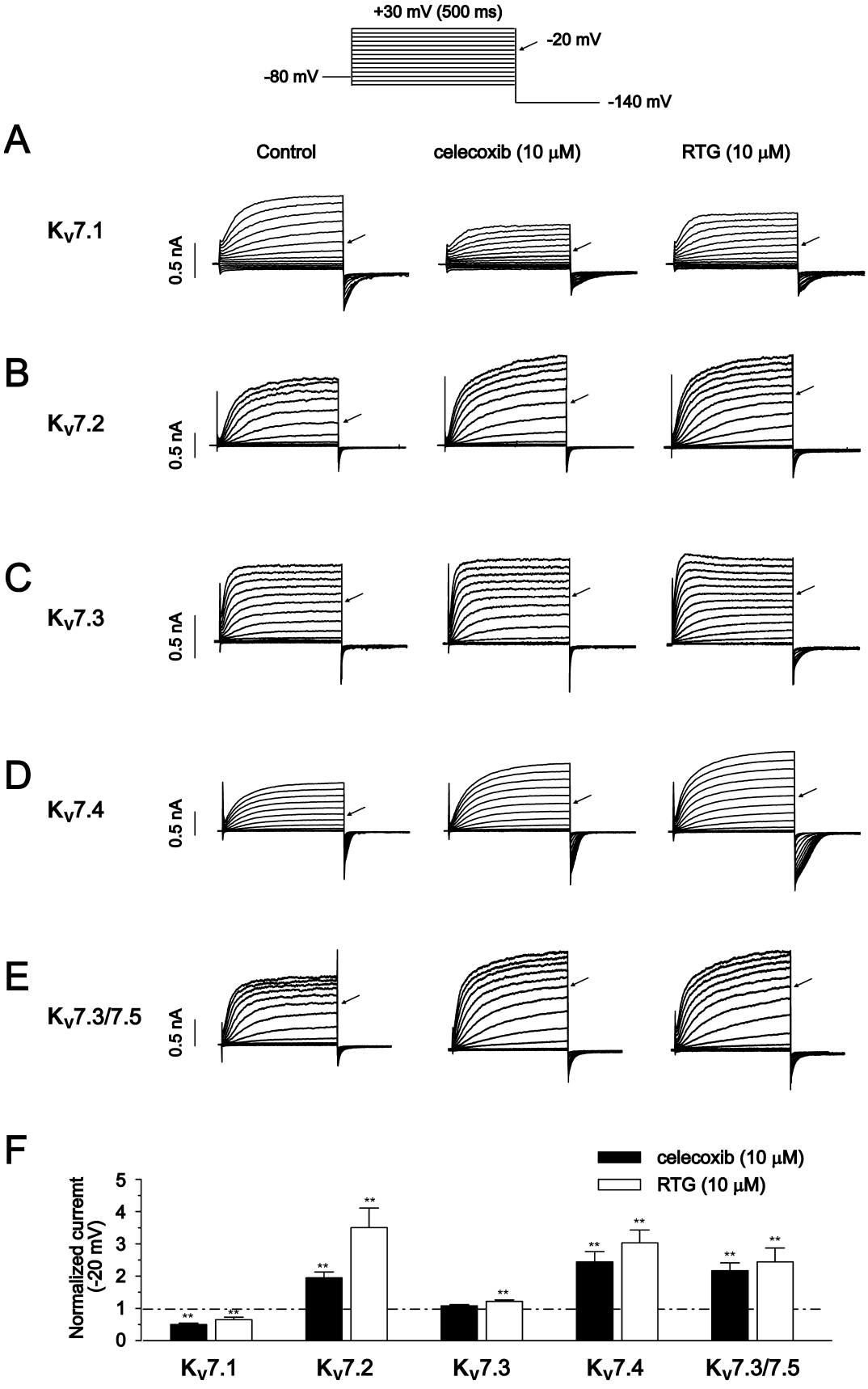
+30 mV (500 ms)
-20 mV
-80 mV
-140 mV
A
Control
celecoxib (10 μM)
RTG (10 μM)
KV7.1
0.5 nA
B
KV7.2
0.5 nA
C
KV7.3
0.5 nA
D
KV7.4
0.5 nA
E
KV7.3/7.5
0.5 nA
F
celecoxib (10 μM)
RTG (10 μM)
Normalized curremt (-20 mV)
0
1
2
3
4
5
**
KV7.1
KV7.2
KV7.3
KV7.4
KV7.3/7.5

system was a homemade 100 μL perfusion chamber through which solution flowed continuously at 1–2 mL·min$^{-1}$. Drugs were applied to the cells by gravity via a BPS-8 valve control system (Scientific Instruments). All recordings were carried out at room temperature.

### Homology modelling and docking

The method used for the homology modelling and docking is similar to the method described by Wuttke *et al*. (2005). The MthK channel structure (1LNQ) and the KcsA channel structure (1BL8) were downloaded from the Protein Data Bank (http://www.pdb.org). The three-dimensional structures of the S5 to S6 domains of $K_v$7.2 subunitswere constructed based on the solved crystal structures of the corresponding domains of MthK/KscA. The $K_v$7.2 structures were generated using SWISS-MODEL (Arnold *et al*., 2006; Kiefer *et al*., 2009) and were energy optimized using NAMD (Phillips *et al*., 2005) in default settings. Manual docking of celecoxib and DM-celecoxib molecules which were drawn with Gaussian viewer was performed with Auto dock 4.0.

### Data analysis and statistics

Currents were analysed and fitted using the Clampfit 10 (Axon Instrument) and Origin 7.5 (Originlab Corporation) software. The current amplitudes were measured without leak subtraction and the details were given in the Figure legends. The current activation curves were generated by plotting the normalized tail current amplitudes against the step potentials and were fitted with a Boltzmann function: $y = A/\{1 + \exp[(V_h - V_m)/k]\}$, where A is the amplitude of relationship, $V_h$ is the voltage for half-maximal activation, $V_m$ is the test potential and k is the slope. The kinetics of activation and deactivation were fitted with an exponential function (Clampfit 10): $f(t) = \sum_{i=1}^{n} A_i e^{-t/\tau i} + C$, from which the time constants τ were obtained. Results are expressed as the mean ± SEM. Differences between group means was analysed with one-way ANOVA, followed by the Bonferroni *post hoc* test. The differences were considered significant if $P < 0.05$.

### Materials

Celecoxib, DM-celecoxib and retigabine were synthesized in the Department of New Drug Development, School of Pharmacy, Hebei Medical University. Celecoxib was also purchased from Matrix Scientific (Columbia, SC, USA). The other chemicals were all purchased from Sigma (St. Louis, MO, USA). The stock solutions for celecoxib (100 mM), DM-celecoxib (100 mM) and RTG (100 mM) were made in dimethyl sulphoxide and were stored at –20°C. The celecoxib and RTG solutions were freshly prepared from stock solutions before each experiment and protected from light.

## Results

### Celecoxib inhibits $K_v$7.1 currents and enhances $K_v$7.2–7.4 and $K_v$7.3/ $K_v$7.5 currents

We started our experiments by studying the effects of celecoxib on homomeric $K_v$7.1–7.4 and heteromeric $K_v$7.3/ $K_v$7.5 channels expressed in HEK293 cells. The effects of celecoxib were compared with those of retigabine, a well established $K_v$7 channel opener (Figure S1) (Tatulian *et al*., 2001). Figure 1 shows the current traces of the $K_v$7 channels recorded using the voltage protocol shown at the top of the Figure. Celecoxib affected the $K_v$7 currents in a manner qualitatively similar to retigabine; thus, both drugs inhibited $K_v$7.1 currents while enhancing $K_v$7.2– $K_v$7.4 and $K_v$7.3/ $K_v$7.5 currents (Figure 1). The effects of celecoxib and retigabine were quantified by measuring the changes in the current amplitude at –20 mV induced by the drugs (indicated by the arrows in Figure 1A–E), and the results are summarized in Figure 1F. Both celecoxib and retigabine induced a significant inhibition in $K_v$7.1 currents, but the effect of celecoxib was more substantial (the maximum current at –20 mV was inhibited 50 ± 4% and 35 ± 8% by celecoxib and retigabine respectively ($P < 0.05$). Celecoxib 10 μM also inhibited the $K_v$7.1/KCNE1 currents (currents were reduced by 47 ± 4%, $n = 5$). Similarly, retigabine at 10 μM inhibited $K_v$7.1/KCNE1 currents (Figure S2A), although less than celecoxib (currents were reduced by 29 ± 4%, $n = 5$).

Celecoxib significantly increased the currents of $K_v$7.2 and $K_v$7.4 at –20 mV by 95 ± 18%, and 144 ± 32% respectively (Figure 1F). However, the currents of $K_v$7.3 at –20 mV was not significantly affected (Figure 1F). Although we could sometimes detect the currents of $K_v$7.5 expressed in HEK293 cells and the currents were also enhanced by celecoxib (Figure S2B), the lack of consistency in measurable $K_v$7.5 currents prevented a systematic study on celecoxib modulation of homomeric $K_v$7.5 currents. We encountered the same problem in our previous study (Liu *et al*., 2008). Because we studied the effects of celecoxib in close comparison with retigabine and because most of the information concerning the effects of retigabine is from heteromeric $K_v$7.3/$K_v$7.5 currents (Wickenden *et al*., 2000; Wickenden *et al*., 2001), we characterized the effects of celecoxib on heteromeric $K_v$7.3/ $K_v$7.5 currents instead. As shown in Figure 1E and F, celecoxib increased $K_v$7.3/ $K_v$7.5 currents measured at –20 mV by 117 ± 24%.

I-V curves for voltage-dependent activation of $K_v$7 currents were established from the tail currents at –140 mV, and

**Figure 2**

The effects of celecoxib on the activation and deactivation kinetics of $K_v$7 currents. The activation and deactivation of $K_v$7 currents were recorded by the depolarization step of –20 mV and the repolarization step of –60 mV, respectively, and the protocol was shown at the top of the figure. The amplitudes of the control current traces were either scaled down (for $K_v$7.1 currents in A) or scaled up (for $K_v$7.2–7.5 currents in B–E) to normalize to the amplitudes of $K_v$7 currents in the presence of 10 μM celecoxib. Both activation and deactivation of $K_v$7 currents were fitted with the exponential function described. The time constants from these fittings were shown in the right panel. $n = 5$–6. *$P < 0.05$, **$P < 0.01$ compared with the currents in the absence of celecoxib.

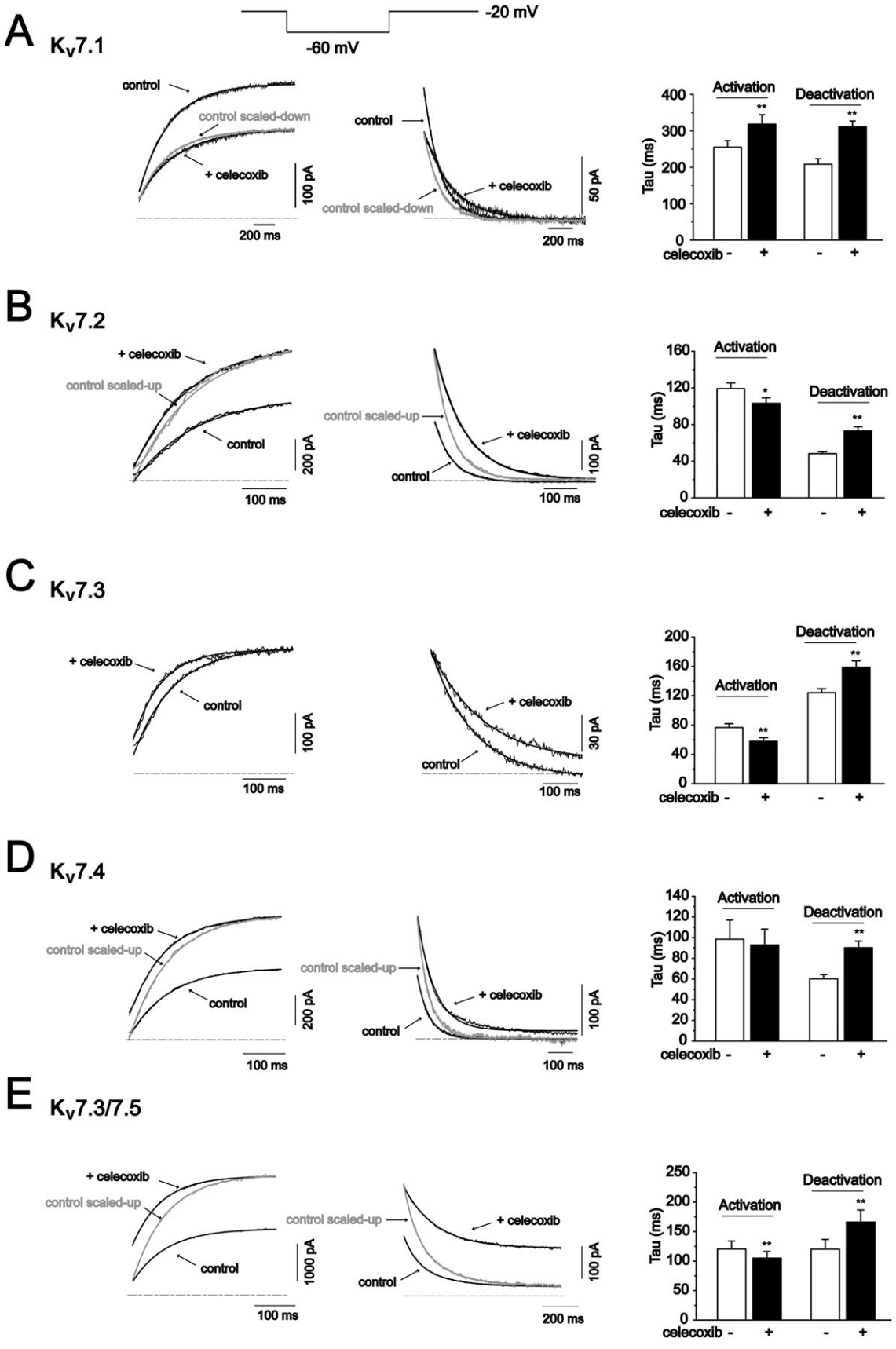
A
Kv7.1
-20 mV
-60 mV
control
control scaled-down
+ celecoxib
100 pA
200 ms
control
+ celecoxib
control scaled-down
50 pA
200 ms
Activation
Deactivation
Tau (ms)
celecoxib - + - +
B
Kv7.2
+ celecoxib
control scaled-up
control
200 pA
100 ms
control scaled-up
+ celecoxib
control
100 pA
100 ms
Activation
Deactivation
Tau (ms)
celecoxib - + - +
C
Kv7.3
+ celecoxib
control
100 pA
100 ms
+ celecoxib
control
30 pA
100 ms
Deactivation
Activation
Tau (ms)
celecoxib - + - +
D
Kv7.4
+ celecoxib
control scaled-up
control
200 pA
100 ms
control scaled-up
+ celecoxib
control
100 pA
100 ms
Activation
Deactivation
Tau (ms)
celecoxib - + - +
E
Kv7.3/7.5
+ celecoxib
control scaled-up
control
1000 pA
100 ms
control scaled-up
+ celecoxib
control
100 pA
200 ms
Activation
Deactivation
Tau (ms)
celecoxib - + - +

the half-activation potential ($V_{1/2}$) was obtained from the fitting functions described in *Methods*. The $V_{1/2}$ changes ($\Delta V_{1/2}$) induced by celecoxib and retigabine are summarized in Table 1. Celecoxib and retigabine did not affect the $V_{1/2}$ of $K_v7.1$ currents (Table 1). By contrast, celecoxib and retigabine significantly shifted the $V_{1/2}$ of $K_v7.2$–7.4 and $K_v7.3/K_v7.5$ currents to more negative potentials (Table 1). However, it is clear from the data shown in Table 1 that retigabine is more effective at negatively shifting the voltage-dependent activation of $K_v7$ currents.

The effects of celecoxib on the activation and deactivation kinetics of $K_v7$ channels were also tested, and the results are shown in Figure 2. The current activation traces induced by the depolarization step to –20 mV and the tail current deactivation traces at –60 mV before and after application of celecoxib are shown. The activation and the deactivation current traces were fitted with exponential functions. Celecoxib slowed the activation of $K_v7.1$ currents (Figure 2A) while enhancing the activation of $K_v7.2$ (Figure 2B), $K_v7.3$ (Figure 2C) and $K_v7.3/K_v7.5$ (Figure 2E); the activation kinetics of $K_v7.4$ channels were not significantly affected (Figure 2D). Celecoxib also slowed the deactivation processes of all $K_v7$ currents (Figure 2A–E, Table 1).

The concentration–response relationship of celecoxib was then established for each of the expressed $K_v7$ channels (Figure 3). For this investigation, $K_v7$ currents activated at –20 mV and –60 mV were measured at different concentrations of celecoxib. The concentration–response curves were constructed from the normalized currents over the control measured at –20 mV. Celecoxib concentration-dependently inhibited $K_v7.1$ currents and enhanced $K_v7.2$, $K_v7.4$ and $K_v7.3/K_v7.5$ currents at –20 mV. Celecoxib affected $K_v7$ currents with similar potency and efficacy. Thus, celecoxib began affecting $K_v7$ currents at approximately 1 μM and reached a maximal effect at approximately 10–30 μM (Figure 3). At the maximal effect, celecoxib inhibited $K_v7.1$ currents by ~60% and increased $K_v7.2$, $K_v7.4$ and $K_v7.3/K_v7.5$ currents by ~100%. The $IC_{50}$ of celecoxib for $K_v7.1$ was 4.00 ± 0.13 μM; and the $EC_{50}$s of celecoxib for $K_v7.2$, $K_v7.4$ and $K_v7.3/K_v7.5$ were 3.09 ± 0.27 μM, 3.37 ± 0.26 μM and 2.27 ± 0.4 μM respectively. Celecoxib did not significantly affect $K_v7.3$ currents when measured at –20 mV (see also Figure 1F), but did concentration-dependently increase the current measured at –60 mV (Figure 3C). This result was consistent with celecoxib not increasing the maximum current amplitude but negatively shifting the voltage-dependent activation of $K_v7.3$ currents, as described above in Table 1.

## *Celecoxib modulates $K_v7$ currents with a mechanism similar to that of retigabine*

Both celecoxib and retigabine inhibited $K_v7.1$ and activate $K_v7.2$– $K_v7.4$ and $K_v7.3/K_v7.5$ currents, and they both negatively shifted the voltage-dependent activation and slowed the deactivation of $K_v7.2$– $K_v7.4$ and $K_v7.3/K_v7.5$ channels. These data suggest that celecoxib may share a mechanism with retigabine for modulating $K_v7$ channel functions. It has been suggested that retigabine opens $K_v7.2$ channels by binding to the channel activation gate (Wuttke *et al.*, 2005). A tryptophan residue at the cytoplasmic end of S5, Trp236, has been suggested as critical for this binding and for activation of the channel. Trp236 is conserved in $K_v7.2$–7.5 but is replaced by a leucine in the case of $K_v7.1$ channels. Mutation of Trp236 to leucine ($K_v7.2$(W236L)) abolished the effects of retigabine on $K_v7.2$ channels (Wuttke *et al.*, 2005). A residue adjacent to Trp236, Ala235, is also conserved in $K_v7.2$–7.5 channels but is replaced by a threonine in the case of $K_v7.1$ channels. This Ala235 seems to play a minor role in the activation of $K_v7.2$ channels by retigabine (Wuttke *et al.*, 2005). We tested the effects of celecoxib on the mutant channels, $K_v7.2$(W236L) and $K_v7.2$(A235T), compared with those of retigabine (Figure 4). For $K_v7.2$(A235T) channels, the stimulatory effect of celecoxib on $K_v7.2$ currents was reversed to become a potent inhibitory effect, whereas the stimulatory effect of retigabine remained (Figure 4A and B). For $K_v7.2$(W236L) channels, the stimulatory effects of both celecoxib and retigabine disappeared, and celecoxib became inhibitory (Figure 4A and C). The effects of celecoxib and retigabine on these two $K_v7.2$ channel mutants were further quantified, as shown in Figure 4B–E. Celecoxib inhibited $K_v7.2$(A235T) and $K_v7.2$(W236L) currents, concentration-dependently (Figure 4B and C). By comparison, celecoxib at 10 μM increased $K_v7.2$ currents by 81 ± 6% and inhibited $K_v7.2$(A235T) currents by 82 ± 3% and $K_v7.2$(W236L) currents by 31 ± 3% (Figure 4E). By contrast, retigabine at 10 μM increased $K_v7.2$ currents by 309 ± 59% and increased $K_v7.2$(A235T) currents by only 49 ± 4% and did not affect $K_v7.2$(W236L) currents (Figure 4E). Thus, as is the case for retigabine, Trp236 in $K_v7.2$ channels is critical for celecoxib-induced activation of the channels.

Unlike wild-type $K_v7.2$, the voltage-dependent activation of $K_v7.2$(W236L) currents was no longer shifted by celecoxib or retigabine (Table 1). Furthermore, the voltage-dependent activation of $K_v7.2$(A235T) currents was positively shifted by celecoxib but was modestly shifted by retigabine towards a more negative potential (Table 1).

## Figure 3

The concentration-dependent effects of celecoxib on $K_v7$ currents. The concentration–response relationships of celecoxib on homomeric $K_v7.1$–7.4 currents (A–D) and heteromeric $K_v7.3/K_v7.5$ (E) were shown. The left panel shows the time courses of concentration-dependent modulation of the $K_v7$ currents recorded at –20 mV (upper line) and –60 mV (lower line). The currents were recorded using the protocol shown in Figure 3. The current amplitudes were measured every 1 s. The right panel shows the fitted curves for the concentration-dependent effects of celecoxib on $K_v7$ currents recorded at –20 mV. The dotted line indicates the control current level before celecoxib application. The concentration–response relationships were fitted with the logistic function. The $IC_{50}$ is 4.00 ± 0.13 μM ($K_v7.1$). The $EC_{50}$ values are 3.09 ± 0.27 μM ($K_v7.2$), 3.37 ± 0.26 μM ($K_v7.4$) and 2.27 ± 0.40 μM ($K_v7.3/K_v7.5$), $n$ = 2–14.

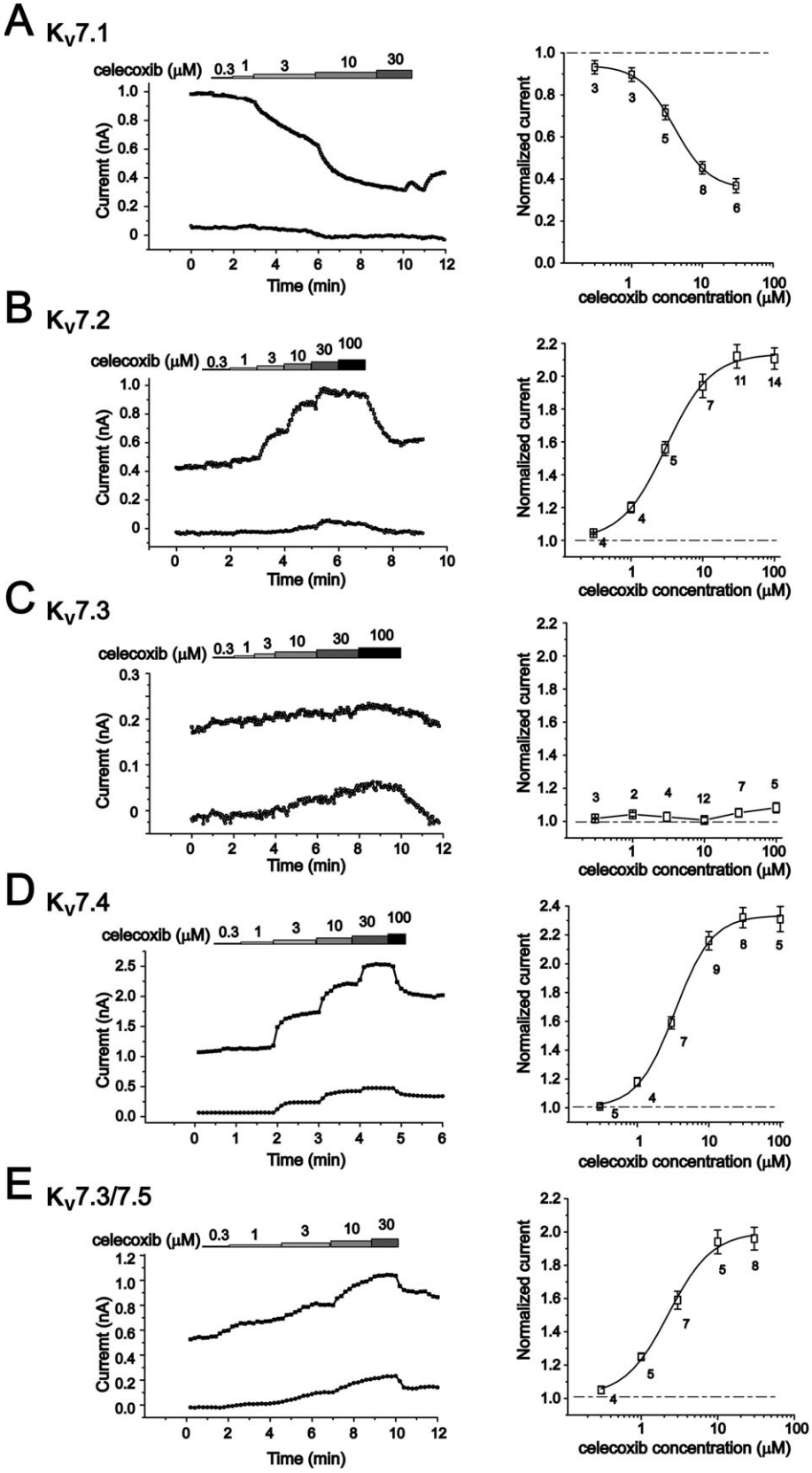
A Kv7.1
celecoxib (μM) 0.3 1 3 10 30
Current (nA)
Time (min)
Normalized current
celecoxib concentration (μM)
B Kv7.2
celecoxib (μM) 0.3 1 3 10 30 100
Current (nA)
Time (min)
Normalized current
celecoxib concentration (μM)
C Kv7.3
celecoxib (μM) 0.3 1 3 10 30 100
Current (nA)
Time (min)
Normalized current
celecoxib concentration (μM)
D Kv7.4
celecoxib (μM) 0.3 1 3 10 30 100
Current (nA)
Time (min)
Normalized current
celecoxib concentration (μM)
E Kv7.3/7.5
celecoxib (μM) 0.3 1 3 10 30
Current (nA)
Time (min)
Normalized current
celecoxib concentration (μM)

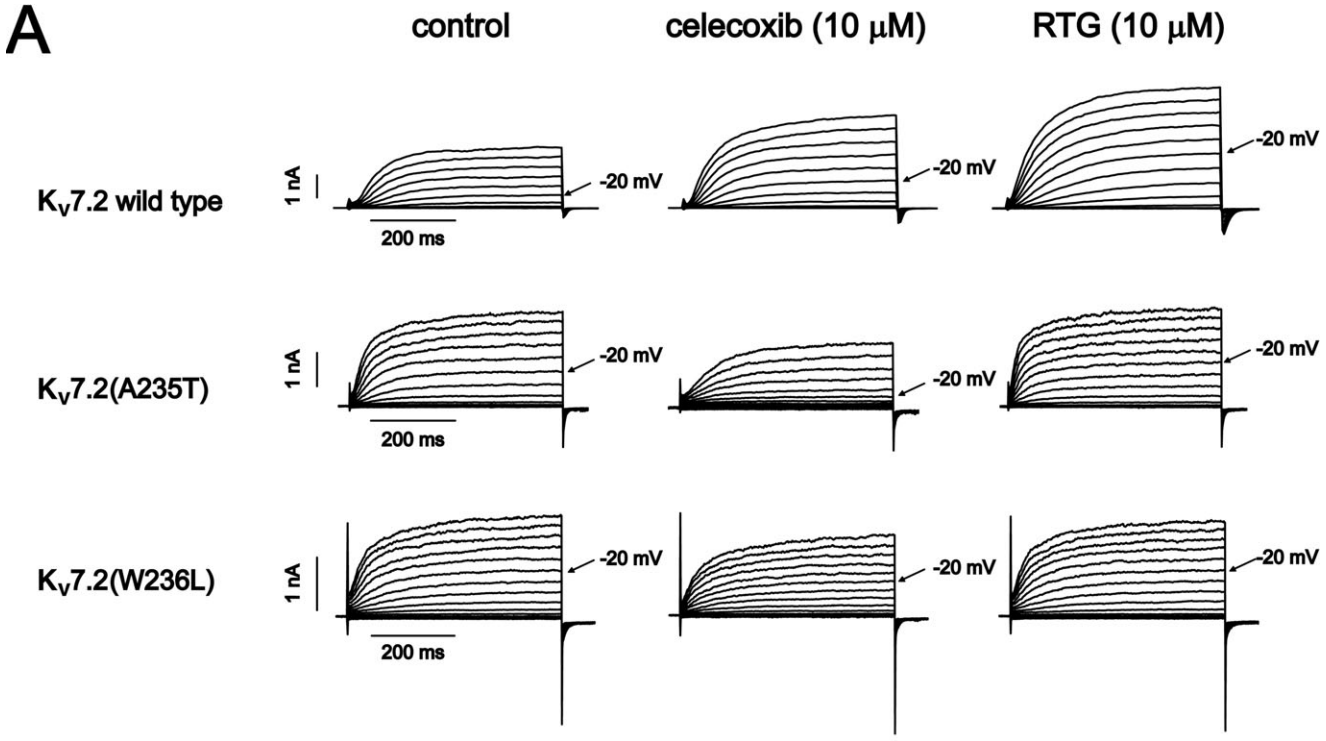
A
control
celecoxib (10 μM)
RTG (10 μM)
Kv7.2 wild type
Kv7.2(A235T)
Kv7.2(W236L)
1 nA
200 ms
-20 mV

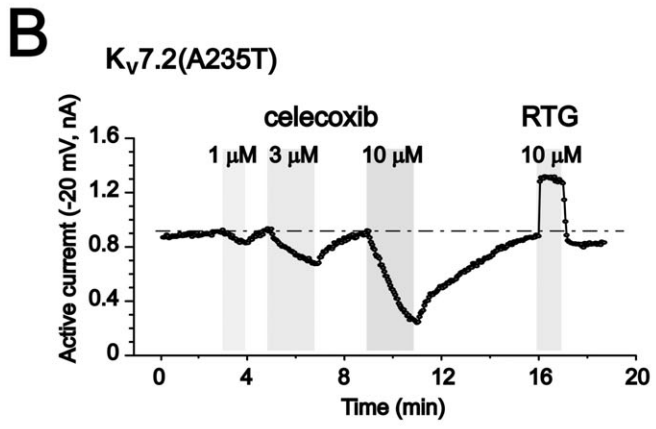
B
Kv7.2(A235T)
celecoxib
RTG
1 μM 3 μM 10 μM
10 μM
Active curremt (-20 mV, nA)
Time (min)

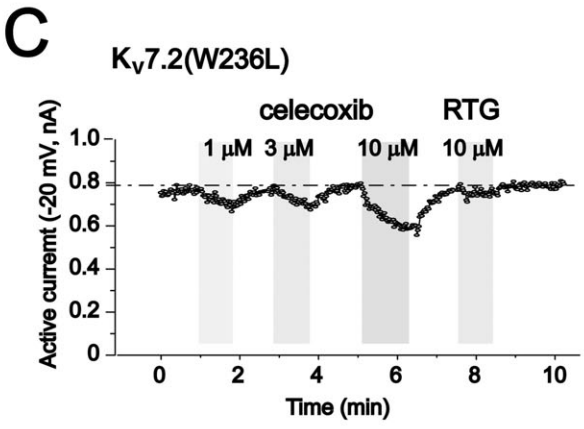
C
Kv7.2(W236L)
celecoxib
RTG
1 μM 3 μM 10 μM
10 μM
Active curremt (-20 mV, nA)
Time (min)

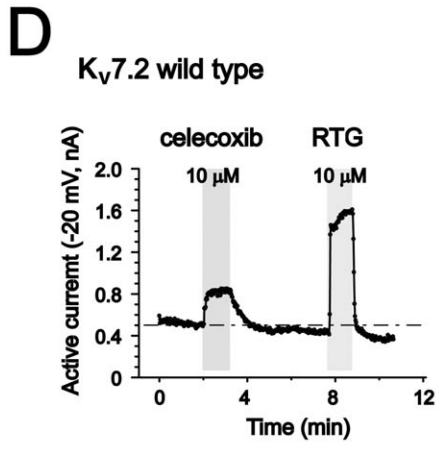
D
Kv7.2 wild type
celecoxib
RTG
10 μM
10 μM
Active curremt (-20 mV, nA)
Time (min)

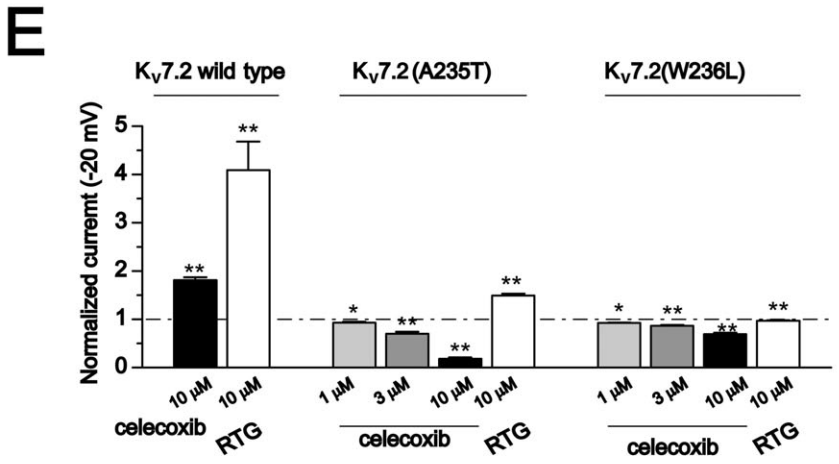
E
Kv7.2 wild type
Kv7.2 (A235T)
Kv7.2(W236L)
Normalized curremt (-20 mV)
10 μM
celecoxib
RTG
1 μM
3 μM

## Figure 4

The effects of celecoxib and retigabine on $K_v7.2$(A235T) and $K_v7.2$(W236L) currents. (A) The current traces of $K_v7.2$, $K_v7.2$(A235T) and $K_v7.2$(W236L) recorded using the voltage protocol shown in Figure 1. The effects of 10 μM celecoxib and 10 μM retigabine (RTG) are shown. (B–D) The time courses for the effects of celecoxib and retigabine on $K_v7.2$(A235T) (B), $K_v7.2$(W236L) (C) and $K_v7.2$ (D) currents recorded at −20 mV. (E) The normalized currents recorded at −20 mV. The control current amplitudes before celecoxib and retigabine application were taken as 1. *$P < 0.05$, **$P < 0.01$ compared with the control currents in the absence of celecoxib or retigabine, $n = 3–8$.

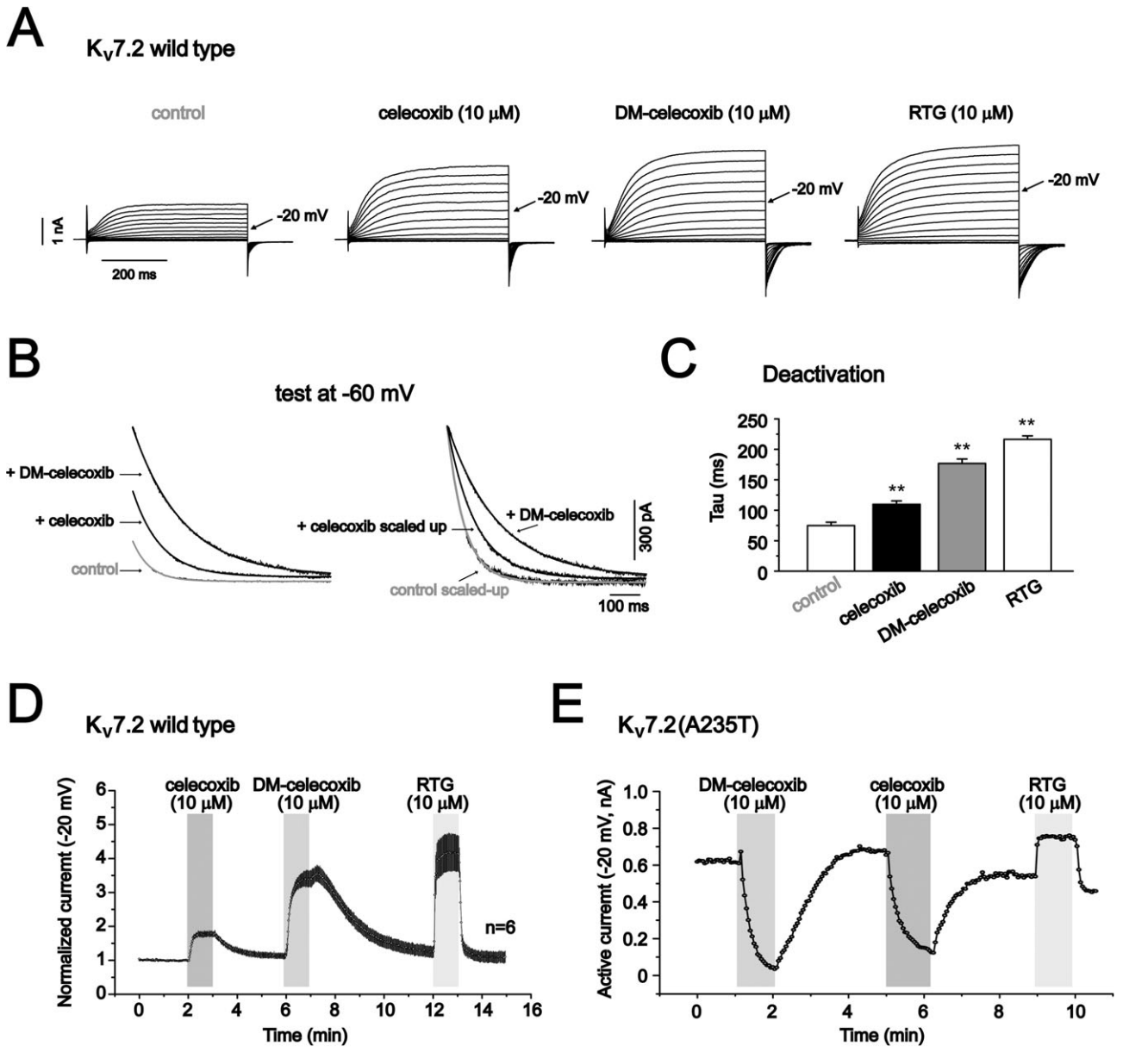


## Figure 5

The effects of DM-celecoxib on $K_v7$ currents. (A) The currents traces of $K_v7.2$ recorded using the voltage protocol shown in Figure 1. The effects of 10 μM celecoxib, 10 μM DM-celecoxib and 10 μM retigabine (RTG) were shown. (B) The effects of celecoxib and DM-celecoxib on the deactivation kinetics of $K_v7.2$ currents recorded at −60 mV (the currents were first activated at −20 mV). The control and the celecoxib-activated currents were normalized based on the currents activated by DM-celecoxib. (C) Summarized data of the deactivation time constants. (D–F) The time courses for the effects of celecoxib, DM-celecoxib and retigabine on $K_v7.2$ (D), $K_v7.2$(A235T) (E) and $K_v7.2$(W236L) (F) currents recorded at −20 mV. Note that the $K_v7.2$ (D) currents were from normalized currents of six recordings. (G) Normalized currents recorded at −20 mV. The control current amplitude before celecoxib, DM-celecoxib and retigabine were taken as 1. *$P < 0.05$, **$P < 0.01$ compared with the control currents in the absence of celecoxib, DM-celecoxib or retigabine, $n = 6–8$.

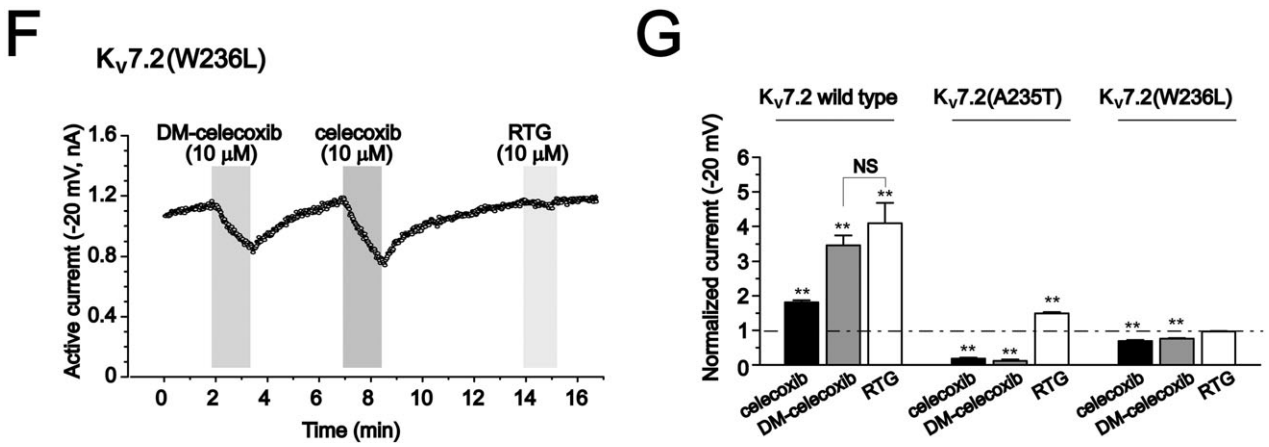


## Figure 5

*Continued.*

## Figure 6

The effects of celecoxib on $K_v$7.2 $K_v$7.3 currents and M-type currents from rat SCG neurons. (A) The currents traces of $K_v$7.2/ $K_v$7.3 recorded using the voltage protocol shown in Figure 1. The effects of 10 μM celecoxib and 10 μM retigabine (RTG) are shown. (B) The effects of celecoxib on the activation and deactivation kinetics of $K_v$7.2/ $K_v$7.3 currents. (C) Summarized data of the activation and deactivation time constants. (D) The time course of concentration-dependent effects of celecoxib on $K_v$7.2/ $K_v$7.3 currents recorded using the protocol shown at the right panel. The current traces at −20 mV (upper line) and −60 mV (lower line) were shown. (E) The fitted curve for the concentration–response effect of celecoxib. The $EC_{50}$ is 4.95 ± 1.16 μM, $n$ = 5–7. (F) M-type currents from rat SCG neurons were recorded using the voltage shown and the effects of different concentration of celecoxib were shown. The M-type currents were measured at −20 mV and the deactivation of the currents were measured at −60 mV. (G) Concentration-dependent activation of M-type currents by celecoxib from SCG neurons. $^{**}P < 0.01$ compared with the currents in the absence of celecoxib. $n$ = 5.

To further evaluate the importance of Ala235 and Trp236 in the effects of celecoxib described above, these residues were introduced into the corresponding sites in $K_v$7.1 channels and the effects of celecoxib and retigabine tested. For $K_v$7.1(L266W) channels, celecoxib and retigabine, both at 10 μM, inhibited the current amplitude recorded at −20 mV by 45 ± 2% ($n$ = 5) and 29 ± 6% ($n$ = 3) respectively, which are similar to celecoxib- and retigabine-induced inhibition of wild-type $K_v$7.1 channels (50 ± 4% and 35 ± 8%, Figure 1F). For the mutant $K_v$7.1 (T265A) channels, celecoxib inhibited the current amplitude recorded at 0 mV by 39 ± 3% ($n$ = 4), whereas retigabine did not inhibit the currents (Figure S3). We measured $K_v$7.1(T265A) currents at 0 mV because it has lower current density than the wild type $K_v$7.1 channels. For comparison, celecoxib and retigabine inhibited wild type $K_v$7.1 currents recorded at 0 mV by 40 ± 7% ($n$ = 4) and 23 ± 4% ($n$ = 4) respectively (Figure S3).

### *The effects of celecoxib on $K_v$7 channels do not depend on its inhibition of COX*

Previous work has shown that DM-celecoxib, a celecoxib analogue that does not inhibit COX-2 (Schonthal *et al.*, 2008), mimics the effects of celecoxib on activation of $K^+$ currents and inhibition of $Ca^{2+}$ currents (Brueggemann *et al.*, 2009). We tested whether DM-celecoxib could also mimic the effects of celecoxib on $K_v$7.2, $K_v$7.2(A235T) and $K_v$7.2(W236L) currents. Indeed, as shown in Figure 5, DM-celecoxib had similar effects to celecoxib on currents in both $K_v$7.2 channels and its mutants. At the same concentration, in fact, DM-celecoxib affected $K_v$7.2 currents to a greater extent than did celecoxib (Figure 5A). The voltage-dependent activation was further shifted to more negative potentials (−22.5 ± 1.9 mV, $n$ = 3), and the deactivation kinetics were further slowed (Figure 5B and C). Actually, the effects of DM-celecoxib were closer to those of retigabine than those of celecoxib, with respect to the increase of the current amplitude (Figure 5A, D and G), the shifting of voltage-dependent activation and the slowing of the deactivation processes (Figure 5B and C).

Importantly, DM-celecoxib affected $K_v$7.2(A235T) and $K_v$7.2(W236L) currents in a manner similar to celecoxib (Figure 5E–G). Also, in both $K_v$7.2(A235T) and $K_v$7.2(W236L) channels, the effects of DM-celecoxib were reversed from activation to inhibition (Figure 5E and F). DM-celecoxib and celecoxib inhibited $K_v$7.2(A235T) and $K_v$7.2(W236L) currents to a similar extent (Figure 5G).

### *The effects of celecoxib on $K_v$7/M-type currents*

We then examined whether celecoxib could also modulate native $K_v$7 currents. The $K_v$7 currents in neuronal cells are best manifested by the M-type currents found in these cells. M-type currents from sympathetic neurons (Brown and Adams, 1980) have been used extensively for the study of M/$K_v$7 channel modulations. M-channels are most likely

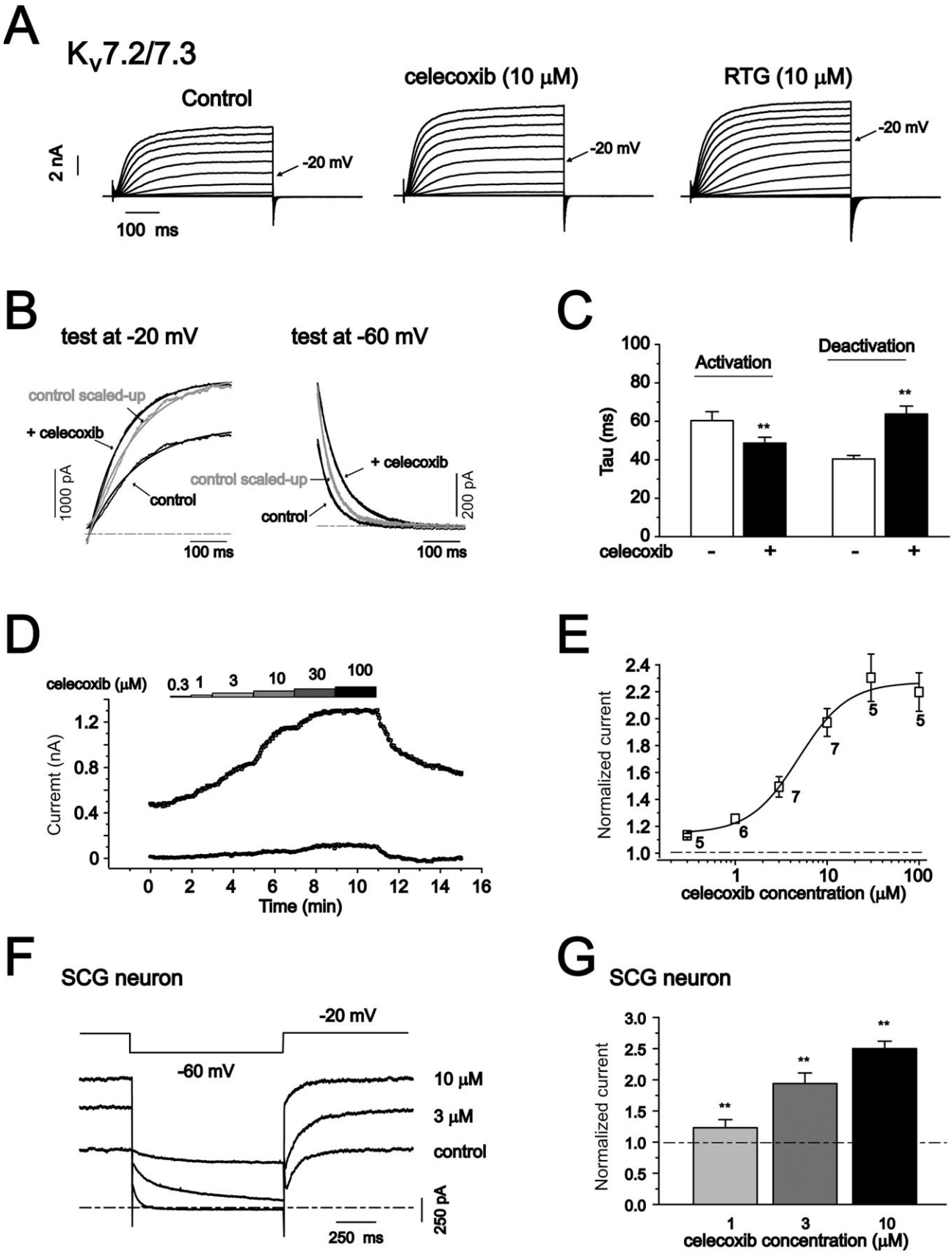
A
$K_V$7.2/7.3
Control
celecoxib (10 μM)
RTG (10 μM)
2 nA
-20 mV
100 ms
B
test at -20 mV
test at -60 mV
control scaled-up
+ celecoxib
control
1000 pA
200 pA
100 ms
C
Activation
Deactivation
Tau (ms)
celecoxib
D
celecoxib (μM)
0.3 1 3 10 30 100
Curremt (nA)
Time (min)
E
Normalized current
celecoxib concentration (μM)
F
SCG neuron
-20 mV
-60 mV
10 μM
3 μM
control
250 pA
250 ms
G
SCG neuron
Normalized current
celecoxib concentration (μM)

composed of $K_v7.2$ and $K_v7.3$ subunits (Wang *et al.*, 1998; Hadley *et al.*, 2000; Shapiro *et al.*, 2000). Thus, we first tested the effects of celecoxib on heteromeric $K_v7.2/K_v7.3$ currents expressed in HEK293 cells. Celecoxib at 10 μM slightly increased the maximal amplitude of $K_v7.2/K_v7.3$ currents (Figure 6A), but significantly shifted the voltage-dependent activation of $K_v7.2/K_v7.3$ currents (Table 1). Similar to other $K_v7$ currents, the deactivation of $K_v7.2/K_v7.3$ currents was also significantly slowed, and the activation was mildly enhanced (Figure 6B and C, Table 1). Celecoxib increased $K_v7.2/K_v7.3$ currents in a concentration-dependent manner (Figure 6D) with an $EC_{50}$ of 4.95 ± 1.16 μM (Figure 6E).

The effects of celecoxib on the native M-type currents were tested on neurons from rat SCG using the protocol shown at the top of Figure 6F (Adams *et al.*, 1982). Celecoxib enhanced M-type currents in a concentration-dependent manner (Figure 6F and G). At 10 μM, celecoxib increased M-type currents (at –20 mV) by 154 ± 24% (Figure 6G). As for the expressed $K_v7.2/K_v7.3$ currents, celecoxib also slowed the deactivation of M-type currents. The time constants of current deactivation at –60 mV were 61.2 ± 13.1 ms ($n$ = 4) and 217.2 ± 74.5 ms ($n$ = 4, $P < 0.01$ compared with the control) for control and celecoxib 10 μM respectively.

## Discussion and conclusions

In the present study, we have characterized the effects of celecoxib on the homomeric $K_v7.2$–7.4 and heteromeric $K_v7.2/ K_v7.3$, $K_v7.3/ K_v7.5$ currents of $K_v7$ channels and on the native neuronal M/ $K_v7$ currents. The results demonstrate that all $K_v7$ channels are targets for modulation by celecoxib. Importantly, celecoxib shares a similar mechanism of action with retigabine but also utilizes a distinct mechanism of its own.

In a previous report, Brueggemann and colleagues suggested that celecoxib can activate $K_v7$ currents (possibly $K_v7.5$) in smooth muscle cells (Brueggemann *et al.*, 2009). However, it was not clear whether celecoxib modulates all $K_v7$ channels or affects $K_v7$ channels in an isoform-specific manner. It was also not clear how the $K_v7$ channels are modulated by celecoxib. We planned our experiments to use retigabine in parallel with celecoxib throughout the investigations to better understand the effects of celecoxib. The effects of retigabine on expressed $K_v7$ currents and native M-type currents have been well characterized (Wickenden *et al.*, 2000; Tatulian *et al.*, 2001; Wickenden *et al.*, 2001; Wuttke *et al.*, 2005). Our results with retigabine are generally in agreement with published data. The outstanding features of retigabine's effects on $K_v7$ currents (with the exception of $K_v7.1$) include negatively shifting voltage-dependent activation and slowing deactivation of $K_v7$ currents (Tatulian *et al.*, 2001). In this regard, the effects of celecoxib are similar to those of retigabine. Celecoxib also produced a negative shifting of voltage-dependent activation and a slowing of current deactivation for $K_v7.2$–7.4, $K_v7.2/ K_v7.3$ and $K_v7.3/ K_v7.5$ (Table 1). As has been previously reported for retigabine (Tatulian *et al.*, 2001), neither retigabine nor celecoxib altered the voltage-dependent activation of $K_v7.1$ currents (Table 1). We also found that both celecoxib and retigabine inhibited $K_v7.1$ current amplitudes (Figure 1). Thus, in general, the effects of celecoxib on $K_v7$ currents were qualitatively similar to those of retigabine.

Apart from the effects on the voltage-dependent activation and the deactivation kinetics, we also found that both retigabine and celecoxib enhanced the maximal current amplitudes of $K_v7.2$, $K_v7.4$ and $K_v7.5$, but not $K_v7.3$ channels. These results were different from those of a previous report, which showed retigabine enhancing the maximal current amplitude from $K_v7.3$ and $K_v7.4$, but not $K_v7.2$ channels (Tatulian *et al.*, 2001). It is not clear what caused this discrepancy, but the different expression systems used (CHO vs. HEK cells) could be one possibility. Nevertheless, celecoxib and retigabine still shared a similar pattern of effects on the maximal currents amplitudes in the present study.

Our results provide the first insight into the mechanism of celecoxib modulation of $K_v7$ channels. It is almost certain that Trp236 in $K_v7.2$, and very likely in all of $K_v7.2$–7.5 channels (as Trp236 is conserved in all these channel proteins), serves as the binding site for retigabine and celecoxib because the mutant channel $K_v7.2$(W236L) was not activated by retigabine and celecoxib and was in fact modestly inhibited by celecoxib (Figure 4, Table 1). It has been suggested that retigabine can bind to the cytoplasmic sites of the S5 and S6 segments of $K_v7.2$ channels and that these bindings involve Trp236 in S5 and the gating hinge Gly301 in S6 (Wuttke *et al.*, 2005). These binding sites would favour $K_v7.2$ channels being in the open conformation, as manifested by the negatively shifted voltage-dependent activation, the slowing of the deactivation and the increased current amplitude, which are shared effects of both retigabine and celecoxib. Our docking simulation results shown in Figure 7 further support that celecoxib and retigabine share a similar mechanism for activation of $K_v7$ channels. The docking modelling suggests that although the binding energies for both celecoxib and DM-celecoxib to closed and open conformations of $K_v7.2$ channels are not very different, celecoxib or DM-celecoxib can form hydrogen bonds with open $K_v7.2$ channels more easily than with closed $K_v7.2$ channels. Thus, at open state, residues Trp236, Gly239 and Phe304 of $K_v7.2$ channels form five hydrogen bonds with celecoxib and seven hydrogen bonds with DM-celecoxib. By contrast, at closed state, only the Phe305 of $K_v7.2$ channels forms one hydrogen bond with DM-celecoxib (Figure 7). Thus, as suggested previously for retigabine, Trp236 is indeed also a binding site for celecoxib and DM-celecoxib at the open state of $K_v7.2$ channels. Our docking results do not suggest a direct interaction between Gly301 of $K_v7.2$ channels with celecoxib. However, Phe304 of the $K_v7.2$ channel, which has been proposed as important for the sensitivity of $K_v7.2$ channels to retigabine (Wuttke *et al.*, 2005), does interact with celecoxib in our simulation. Thus, as suggested by Wuttke *et al.* (2005) for retigabine, celecoxib (and DM-celecoxib) are likely to form a interaction complex with $K_v7.2$ channels in the open conformation, involving some residues around Trp236 of S5 and around the gating hinge (S301) of S6. Introducing Trp236 into $K_v7.1$ channels did not allow these channels to be activated by celecoxib; instead, $K_v7.1$(L266W) currents

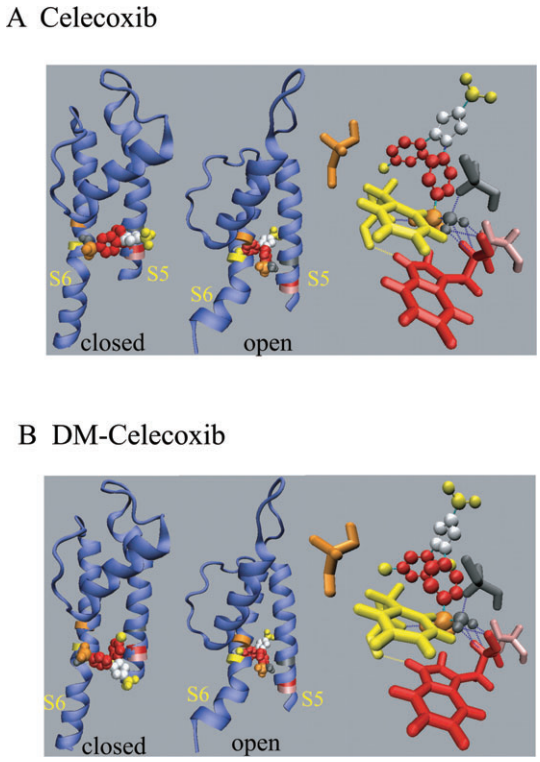


## Figure 7

Docking results for the interaction of celecoxib or DM-celecoxib with residues within S5 and S6 of the $K_v7.2$ channel. Docking results for celecoxib (A) and DM-celecoxib (B) binding to $K_v7.2$ channels. The closed and the open conformations of S5 and S6 segments with the pore loop were shown. The right panel shows the hydrogen bonds (blue dotted lines) between celecoxib (A), DM-celecoxib (B) and W236, G239 and F304 in open channel state. Residues A235, W236, G239, G301, F304 are shown in pink, red, gray, orange and yellow colour respectively. For the structure of celecoxib and DM-celecoxib (see Figure S1), $-CF_3$, benzene, $-SO_2$, $-NH_2$ are shown as yellow, red, orange and gray spheres respectively. The five-carbon ring is shown as silver spheres. Methyls in the benzene are shown as yellow spheres.

were still inhibited by celecoxib, with to the same extent as the wild type $K_v7.1$ currents These results are consistent with the previous work (Wuttke *et al.*, 2005). The overall pore structure of $K_v7.1$ channels might be quite different from $K_v7.2$ channels, and introduction of a single amino acid may not be sufficient to induce celecoxib activation of $K_v7.1$ channels, as observed and suggested by Wuttke *et al.* (2005) for retigabine.

However, it should be noted that there are some distinct differences between celecoxib and retigabine. It is clear that celecoxib has much stronger inhibitory effects on $K_v7$ 1 (and $K_v7.1$/KCNE1) currents than retigabine, while it has weaker stimulatory effects on $K_v7.2$–7.5 currents than retigabine. Furthermore, the experiments with $K_v7.2$(A235T) further suggest a difference between celecoxib and retigabine, as retigabine still enhanced $K_v7.2$(A235T) currents and negatively shifted voltage-dependent activation, whereas celecoxib profoundly inhibited $K_v7.2$(A235T) currents and positively shifted the voltage-dependent activation. Because celecoxib inhibited potently both $K_v7.1$ and $K_v7.2$(A235T) currents, we thought that the Thr265 residue in $K_v7.1$ channels might be the crucial amino acid for celecoxib-induced inhibition. However, celecoxib still inhibited $K_v7.1$(T265A) currents, as well as it did the wild type $K_v7.1$ currents (Figure S3). Interestingly, contrary to wild-type $K_v7.1$, the mutant $K_v7.1$(T265A) channels were no longer inhibited by retigabine (Figure S3). These results suggest that Thr265 did play some role in $K_v7.1$ channel inhibition (at least for retigabine), and the results also indicate there are some other sites which are also involved in celecoxib-mediated inhibition of $K_v7.1$ channels.

It is interesting to note that the celecoxib analogue DM-celecoxib, which has no COX-inhibition activity, has similar activity in regulating activity of $K_v7$ channels. If there is any difference between DM-celecoxib and celecoxib, it is that the former is a stronger activator of $K_v7$ channel functions (Figure 5). It is clear that DM-celecoxib utilizes the same sites for modulating $K_v7$ channels as described above for celecoxib (Figures 5 and 7). Thus, it is likely that the difference in potency between DM-celecoxib and celecoxib in their modulation of $K_v7$ channels arises from their different abilities to interact with the $K_v7$ channel structures, at sites such as Ala235 and Trp236 in the $K_v7.2$ subunit, which could be the result of the subtle structural differences between DM-celecoxib and celecoxib (Figure S1). However, our docking modelling work did not give a clear explanation for the differences between celecoxib and DM-celecoxib. The methyls in the benzene ring (the numbers and the positions are different between celecoxib and DM-celecoxib, Figure S1) are not involved in the direct interaction with residues of $K_v7.2$ channels (Figure 7) and the orientation of two small molecules within $K_v7.2$ channels is similar (Figure 7). Anyway, the quantitative functional difference between celecoxib and DM-celecoxib may be too small to be resolved by the docking modelling in this present study.

These results provide a new template for developing new modulators for $K_v7$ channels and provide a new dimension to the study of COX inhibitors and the structure–function relationship of $K_v7$ and other ion channels. Celecoxib and DM-celecoxib are being investigated for their therapeutic potentials as anticancer agents (Schonthal *et al.*, 2008). Intriguingly, the two pharmacological effects, inhibition of COX-2 and suppression of tumour growth, were found to reside in different structural aspects of the celecoxib molecule; therefore, they could be separated. It will also be interesting to see whether the modulatory effects of celecoxib and its analogue on ion channels contribute to their anticancer activity (Brueggemann *et al.*, 2010).

Finally, what are the physiological implications of the present study? The concentrations at which celecoxib modulates $K_v7$ channel functions could be clinically relevant. At a therapeutic dose of 200 mg, the peak plasma concentration of celecoxib in healthy adults is around 2 μM (Davies *et al.*, 2000). Clearly, celecoxib at this concentration significantly affected $K_v7$ channels (Figure 3). Thus, the selective modulation of the $K_v7$ channels expressed in the vascular system ($K_v7.4$, $K_v7.5$) (Yeung *et al.*, 2007; Zhong *et al.*, 2010) by celecoxib, but not by rofecoxib, may underlie their different cardiovascular side effects (Shapiro, 2009; Brueggemann *et al.*, 2010). $K_v7.2$– $K_v7.5$ channels are expressed in the

nervous system (Jentsch, 2000; Robbins, 2001) and contribute differentially to neuronal M-type currents, depending on the location (Brown and Passmore, 2009). Recently, M/$K_v$7 currents were found to be important for controlling the excitability of sensory neurons related to pain transduction and opening M/$K_v$7 channels can antagonize nociceptive behaviour (Passmore *et al.*, 2003; Linley *et al.*, 2008; Liu *et al.*, 2010). It will be interesting to know whether any analgesic effects of celecoxib could result from the activation of M/$K_v$7channels. Along the same lines, DM-celecoxib, which lacks COX-2 inhibition but has greater $K_v$7 channel activation activity, would be expected to exert analgesic and anti-epileptic effects, similar to those of retigabine, because retigabine has been developed as a new class of anti-epileptic drug. Another intriguing issue raised recently by Zhou *et al.* (2010) is that persistent opening of M/$K_v$7 channels in hippocampal neurons can induce apoptosis of these neurons. In this case, could celecoxib cause neuronal cell death through activation of M/$K_v$7 channels? Considering that celecoxib is already a widely prescribed COX-2 inhibitor and the new potential clinical indications, such as cancer, are being assessed for celecoxib, these issues are worthy of further investigation.

## Acknowledgements

This work was supported by National Natural Science Foundation of China (30730031) to H. Z., (30500112) X. D. and by the 973 Program (2007CB512100) to H. Z. H. Z. was a recipient of National Science Fund for Distinguished Young Scholars of China (30325038). Bingcai Guan read the manuscript and gave valuable suggestions.

## Conflicts of interest

There are no conflicts of interest.

## References

Adams PR, Brown DA, Constanti A (1982). M-currents and other potassium currents in bullfrog sympathetic neurones. J Physiol 330: 537–572.

Alexander SPH, Mathie A, Peters JA (2009). Guide to Receptors and Channels (GRAC), 4th edn. Br J Pharmacol 158 (Suppl. 1): S1–S254.

Arnold K, Bordoli L, Kopp J, Schwede T (2006). The SWISS-MODEL workspace: a web-based environment for protein structure homology modelling. Bioinformatics 22: 195–201.

Aw TJ, Haas SJ, Liew D, Krum H (2005). Meta-analysis of cyclooxygenase-2 inhibitors and their effects on blood pressure. Arch Intern Med 165: 490–496.

Barhanin J, Lesage F, Guillemare E, Fink M, Lazdunski M, Romey G (1996). K(V)LQT1 and lsK (minK) proteins associate to form the I(Ks) cardiac potassium current. Nature 384: 78–80.

Brown DA, Adams PR (1980). Muscarinic suppression of a novel voltage-sensitive K+ current in a vertebrate neurone. Nature 283: 673–676.

Brown DA, Passmore GM (2009). Neural KCNQ (Kv7) channels. Br J Pharmacol 156: 1185–1195.

Brueggemann LI, Mackie AR, Mani BK, Cribbs LL, Byron KL (2009). Differential effects of selective cyclooxygenase-2 inhibitors on vascular smooth muscle ion channels may account for differences in cardiovascular risk profiles. Mol Pharmacol 76: 1053–1061.

Brueggemann LI, Mani BK, Mackie AR, Cribbs LL, Byron KL (2010). Novel actions of nonsteroidal anti-inflammatory drugs on vascular ion channels: accounting for cardiovascular side effects and identifying new therapeutic applications. Mol Cell Pharmacol 2: 15–19.

Cho J, Cooke CE, Proveaux W (2003). A retrospective review of the effect of COX-2 inhibitors on blood pressure change. Am J Ther 10: 311–317.

Davies NM, McLachlan AJ, Day RO, Williams KM (2000). Clinical pharmacokinetics and pharmacodynamics of celecoxib: a selective cyclo-oxygenase-2 inhibitor. Clin Pharmacokinet 38: 225–242.

Flower RJ (2003). The development of COX2 inhibitors. Nat Rev Drug Discov 2: 179–191.

Hadley JK, Noda M, Selyanko AA, Wood IC, Abogadie FC, Brown DA (2000). Differential tetraethylammonium sensitivity of KCNQ1-4 potassium channels. Br J Pharmacol 129: 413–415.

Jentsch TJ (2000). Neuronal KCNQ potassium channels: physiology and role in disease. Nat Rev Neurosci 1: 21–30.

Kiefer F, Arnold K, Kunzli M, Bordoli L, Schwede T (2009). The SWISS-MODEL Repository and associated resources. Nucleic Acids Res 37: D387–D392.

Linley JE, Rose K, Patil M, Robertson B, Akopian AN, Gamper N (2008). Inhibition of M current in sensory neurons by exogenous proteases: a signaling pathway mediating inflammatory nociception. J Neurosci 28: 11240–11249.

Liu B, Zhang X, Wang C, Zhang G, Zhang H (2008). Antihistamine mepyramine directly inhibits KCNQ/M channel and depolarizes rat superior cervical ganglion neurons. Neuropharmacology 54: 629–639.

Liu B, Linley JE, Du X, Zhang X, Ooi L, Zhang H *et al.* (2010). The acute nociceptive signals induced by bradykinin in rat sensory neurons are mediated by inhibition of M-type K+ channels and activation of Ca2+-activated Cl- channels. J Clin Invest 120: 1240–1252.

Mackie AR, Byron KL (2008). Cardiovascular KCNQ (Kv7) potassium channels: physiological regulators and new targets for therapeutic intervention. Mol Pharmacol 74: 1171–1179.

Mackie AR, Brueggemann LI, Henderson KK, Shiels AJ, Cribbs LL, Scrogin KE *et al.* (2008). Vascular KCNQ potassium channels as novel targets for the control of mesenteric artery constriction by vasopressin, based on studies in single cells, pressurized arteries, and in vivo measurements of mesenteric vascular resistance. J Pharmacol Exp Ther 325: 475–483.

McGettigan P, Henry D (2006). Cardiovascular risk and inhibition of cyclooxygenase: a systematic review of the observational studies of selective and nonselective inhibitors of cyclooxygenase 2. JAMA 296: 1633–1644.

Passmore GM, Selyanko AA, Mistry M, Al-Qatari M, Marsh SJ, Matthews EA *et al.* (2003). KCNQ/M currents in sensory neurons: significance for pain therapy. J Neurosci 23: 7227–7236.

Phillips JC, Braun R, Wang W, Gumbart J, Tajkhorshid E, Villa E *et al.* (2005). Scalable molecular dynamics with NAMD. J Comput Chem 26: 1781–1802.

Robbins J (2001). KCNQ potassium channels: physiology, pathophysiology, and pharmacology. Pharmacol Ther 90: 1–19.

Sanguinetti MC, Curran ME, Zou A, Shen J, Spector PS, Atkinson DL *et al.* (1996). Coassembly of K(V)LQT1 and minK (IsK) proteins to form cardiac I(Ks) potassium channel. Nature 384: 80–83.

Schonthal AH, Chen TC, Hofman FM, Louie SG, Petasis NA (2008). Celecoxib analogs that lack COX-2 inhibitory function: preclinical development of novel anticancer drugs. Expert Opin Investig Drugs 17: 197–208.

Shapiro MS (2009). An ion channel hypothesis to explain divergent cardiovascular safety of cyclooxygenase-2 inhibitors: the answer to a hotly debated puzzle? Mol Pharmacol 76: 942–945.

Shapiro MS, Roche JP, Kaftan EJ, Cruzblanca H, Mackie K, Hille B (2000). Reconstitution of muscarinic modulation of the KCNQ2/KCNQ3 K(+) channels that underlie the neuronal M current. J Neurosci 20: 1710–1721.

Tatulian L, Delmas P, Abogadie FC, Brown DA (2001). Activation of expressed KCNQ potassium currents and native neuronal M-type potassium currents by the anti-convulsant drug retigabine. J Neurosci 21: 5535–5545.

Wang HS, Pan Z, Shi W, Brown BS, Wymore RS, Cohen IS *et al.* (1998). KCNQ2 and KCNQ3 potassium channel subunits: molecular correlates of the M-channel. Science 282: 1890–1893.

White WB, West CR, Borer JS, Gorelick PB, Lavange L, Pan SX *et al.* (2007). Risk of cardiovascular events in patients receiving celecoxib: a meta-analysis of randomized clinical trials. Am J Cardiol 99: 91–98.

Wickenden AD, Yu W, Zou A, Jegla T, Wagoner PK (2000). Retigabine, a novel anti-convulsant, enhances activation of KCNQ2/Q3 potassium channels. Mol Pharmacol 58: 591–600.

Wickenden AD, Zou A, Wagoner PK, Jegla T (2001). Characterization of KCNQ5/Q3 potassium channels expressed in mammalian cells. Br J Pharmacol 132: 381–384.

Wuttke TV, Seebohm G, Bail S, Maljevic S, Lerche H (2005). The new anticonvulsant retigabine favors voltage-dependent opening of the Kv7.2 (KCNQ2) channel by binding to its activation gate. Mol Pharmacol 67: 1009–1017.

Yeung SY, Pucovsky V, Moffatt JD, Saldanha L, Schwake M, Ohya S *et al.* (2007). Molecular expression and pharmacological identification of a role for K(v)7 channels in murine vascular reactivity. Br J Pharmacol 151: 758–770.

Zhong XZ, Harhun MI, Olesen SP, Ohya S, Moffatt JD, Cole WC *et al.* (2010). Participation of KCNQ (Kv7) potassium channels in myogenic control of cerebral arterial diameter. J Physiol 588: 3277–3293.

Zhou X, Wei J, Song M, Francis K, Yu SP (2010). Novel role of KCNQ2/3 channels in regulating neuronal cell viability. Cell Death Differ 18: 493–505.

## Supporting information

Additional Supporting Information may be found in the online version of this article:

**Figure S1** The structures of celecoxib, DM-celecoxib and RTG.

**Figure S2** The effects of celecoxib on Kv7.1/KCNEE1 and Kv7.5 currents expressed in HEK 293 cells. (A) The whole-cell currents were recorded from HEK293 cells expressing Kv7.1/E1 with the protocol shown in the inset. The time course of celecoxib and retigabine effects on Kv7.1/E1 tail currents recorded at –40 mV was shown. The percentage inhibition of Kv7.1/E1 currents induced by celecoxib and retigabine was shown in the right panel. (B) The effects of celecoxib on currents of KV7.5 expressed in HEK293. The whole-cell currents were recorded using the voltage protocol shown in Figure 1.

**Figure S3** The effects of celecoxib and retigabine on Kv7.1(T265A) currents. (A) The current traces of Kv7.1, Kv7.1(T265A) recorded using the voltage protocol shown in Figure 1. The effects of 10 μM celecoxib and 10 μM retigabine were shown. (B) The summarized data for the percentage inhibition of Kv7.1 and Kv7.1(T265A) currents recorded at 0 mV. $^{**}P < 0.01$ compared with the control currents in the absence of celecoxib or RTG, $n = 3–5$.

Please note: Wiley-Blackwell are not responsible for the content or functionality of any supporting materials supplied by the authors. Any queries (other than missing material) should be directed to the corresponding author for the article.